

**Widespread evidence for high-temperature formation of pentlandite in chondrites.** D. L. Schrader<sup>1</sup>, T. J. McCoy<sup>1</sup>, and J. Davidson<sup>2</sup>. <sup>1</sup> NMNH, Smithsonian Institution, Washington, DC 20560-0119, USA. <sup>2</sup>DTM, Carnegie Institution of Washington, Washington, DC 20015, USA. email: schraderd@si.edu

### Introduction:

Pentlandite [(Fe,Ni)<sub>9</sub>S<sub>8</sub>] can form via (1) cooling of a primary high temperature Ni-rich Fe-Ni-S melt (pentlandite starts to exsolve ~610°C); (2) thermal metamorphism of a Fe-Ni-S assemblage >610°C and subsequent cooling; (3) annealing between ~600–230°C; and (4) aqueous alteration [e.g., 1–5].

Typically, pentlandite is attributed to forming via parent body aqueous alteration, as suggested for the CI, CM, CR, and CV chondrites and the LL3.00 chondrite Semarkona [e.g., 1,6]. Evidence for this view includes the composition of pentlandite within the CI chondrites, which is consistent with formation during aqueous alteration between 100–135°C [7].

In contrast, experimental petrology shows that pentlandite can also form during the cooling of high temperature Fe-Ni-S melts by exsolution below 610°C during the breakdown of crystallized monosulfide solid solution into pentlandite and pyrrhotite [(Fe,Ni,Co,Cr)<sub>1-x</sub>S] [e.g., 2–4]. When cooling from a melt, pentlandite exsolution commences at ~610–550°C and completes at ~325–275°C [2–4]. Annealing/quench experiments result in rapid (~1 hr) initial exsolution of pentlandite at 500–300°C, however pyrrhotite remained Ni-rich (~17 at.% Ni) after months at constant temperature [4], indicating the formation of intergrowths of pentlandite and Ni-poor pyrrhotite by annealing requires much longer timescales. For instance, annealing Fe-Ni-S mixtures at 230°C over 203 days formed assemblages of pentlandite and Ni-rich pyrrhotite [5].

These mechanisms produce three general morphologies: (1) pentlandite rims around pyrrhotite; (2) blocky pentlandite, which sometimes contain 'islands' of pyrrhotite; and (3) blebs or 'stringers' (often termed flame or brush texture) of pentlandite within pyrrhotite [e.g., 3]. Rapid cooling (quench) results in randomly oriented pentlandite blebs in pyrrhotite, while slower cooling results in oriented blebs and pentlandite lamellae [3].

To critically evaluate the formation conditions of pentlandite within meteorites, we investigated pentlandite and associated sulfides in a brachinite, and the R, LL, CK, and CM chondrites.

### Samples and analytical procedure:

Sulfides in thin sections of 16 meteorites covering a wide range of thermal and aqueous histories were studied: Semarkona USNM1805-17 (LL3.00), Soko-Banja USNM3078-1 (LL4), Siena USNM3070-3 (LL5), Saint-Séverin USNM2608-3 (LL6), MET 01149,27 (R3), LAP 03639,2 (R4), LAP 031275,2 (R5), MIL 11207,2 (R6), LAP 04840,4

(R6), EET 99402,6 (brachinite), Mighei USNM3483-3 (CM2), Sutter's Mill (C, CM-like), Karoonda USNM2428-3 (CK4), ALH 85002,87 (CK4), LAR 06868 (CK5), and LEW 87009 (CK6). Sections were studied via optical microscopy, an FEI Nova NanoSEM 600 scanning electron microscope, and a JEOL 8900 Superprobe electron probe microanalyzer at the Smithsonian Institution.

### Results and Discussion:

The morphology and composition of sulfides vary between meteorite groups (Fig. 1) and petrographic subtype within groups.

*LL chondrites:* Pentlandite (16.0–23.7 wt.% Ni) was observed in each LL chondrite studied and is present as all three textural types (Fig. 1a). It is present as lamellae within pyrrhotite only in Semarkona. The compositions of sulfides are consistent with 600–400°C isothermal phase diagrams. These temperatures are higher than the peak metamorphic temperature inferred for Semarkona [<220°C; 8], but agree with pentlandite formation during cooling after thermal metamorphism for the LL4-6 chondrites [~600–900°C; 9,10]. This is in contrast with the conclusion that pentlandite within Semarkona is solely an aqueous product [6]. This suggests two possibilities: (1) pentlandite within Semarkona is primary (i.e., formed at high temperature during chondrule cooling as in the CR chondrites [11]), or less likely, (2) Semarkona experienced brief high-temperature (600–400°C) sulfide equilibration that did not affect other diffusion-driven geothermometers (e.g., graphite ordering; ol-chr equilibration). Formation of pentlandite lamellae and blebs in an LL impact melt by annealing was suggested by [12].

*R chondrites:* Pentlandite (19.1–38.6 wt.% Ni) is common in the R chondrites and is present as blocky grains, lamellae and oriented blebs within Ni-poor pyrrhotite. The compositions of sulfides in the R chondrites are consistent with 600–400°C isothermal phase diagrams and formation during retrograde metamorphism. Metamorphic temperatures for R chondrites are poorly constrained, with an estimate for the R6 chondrite LAP 04840 of ~670°C [13].

*Brachinite:* Pentlandite (18.9–19.6 wt.% Ni) is rare in the brachinite and is present as lamellae and blebs within Ni-poor pyrrhotite (Fig. 1b). The compositions of sulfides in the brachinite is consistent with 600–400°C isothermal phase diagrams and formation during partial melting for these meteorites at temperatures in excess of 980°C [14].

*CM chondrites:* Pentlandite (22.2–35.0 wt.%

Ni) is common in the CM chondrites and is present as blocky grains, lamellae and oriented blebs within Ni-poor pyrrhotite. While the CM chondrites have experienced extensive 'low-temperature' aqueous alteration (<220°C for Mighei [8], 150–400°C for Sutter's Mill [15]), the compositions of their sulfides are consistent with 600–100°C isothermal phase diagrams. These results are in contrast to the common conclusion that pentlandite in the CM chondrites is solely an aqueous product [e.g., 1,16]. Sulfide textures are often inconsistent with aqueous alteration, in agreement with [17], and the equilibration temperatures indicate formation during cooling from high-temperature; perhaps during chondrule cooling. However, since some sulfides agree with the 100–135°C phase diagram, the formation of some pentlandite via aqueous alteration cannot be ruled out, although low-temperature thermal metamorphism is also possible.

**CK chondrites:** Pentlandite (15.7–41.8 wt.% Ni) is the dominant sulfide in the CK chondrites, and is present as lamellae within pyrite [FeS<sub>2</sub>] and blocky grains with islands of pyrite (Fig. 1c). The compositions of sulfides in the CK chondrites are consistent with 500–230°C isothermal phase diagrams and the conclusions of [18] that the pentlandite-pyrrhotite/ pyrite in the CK4-6 chondrites formed during cooling from peak thermal metamorphic temperatures of 550–950°C, mostly during annealing <300°C.

#### Conclusions:

The combined morphology, composition, and petrographic setting of pyrrhotite-pentlandite intergrowths can be utilized to constrain their formation mechanism. The sulfide equilibration temperatures and the morphology of pentlandite (e.g., lamellae) are consistent with high temperature formation, not low-temperature aqueous alteration. The pentlandite in these samples either formed during cooling after primary formation, or cooling after thermal metamorphism >610°C.

#### References:

[1] Brearley A. J. (2006) *MESS II*, 587–624. [2] Kullerud G. (1963) *Can. Min.* 7, 353–366. [3] Francis C. A. et al. (1976) *Am. Min.* 61, 913–920. [4] Etschmann B. et al. (2004) *Am. Min.* 89, 39–50. [5] Misra K. C. and Fleet M. E. (1973) *Econ. Geo.* 68, 518–539. [6] Rubin A. E. (2006) *MAPS* 41, 1027–1038. [7] Bullock E. S. et al. (2005) *GCA* 69, 2687–2700. [8] Busemann H. et al. (2007) *MAPS* 42, 1387–1416. [9] McCoy T. J. et al. (1991) *GCA* 55, 601–619. [10] Slater-Reynolds V. and McSween H. Y. (2005) *MAPS* 40, 745–754. [11] Schrader D. L. et al. (2010) *LPSC XLI*, 1262. [12] Jamsja N. and Ruzicka A. (2010) *MAPS* 45, 828–849. [13] McCanta M. C. et al. (2008) *GCA* 72, 5757–5780. [14] Gardner-Vandy K. G. et al. (2013) *GCA* 122, 36–57. [15] Jenniskens P. et al. (2012) *Science* 338, 1583–1587. [16] Zolensky M. and Le L. (2003) *LPSC XXXIV*, 1235. [17] Brearley A. J. and Martinez

C. (2010) *LPSC XLI*, 1689. [18] Geiger T. and Bischoff A. (1995) *PSS* 43, 485–498.

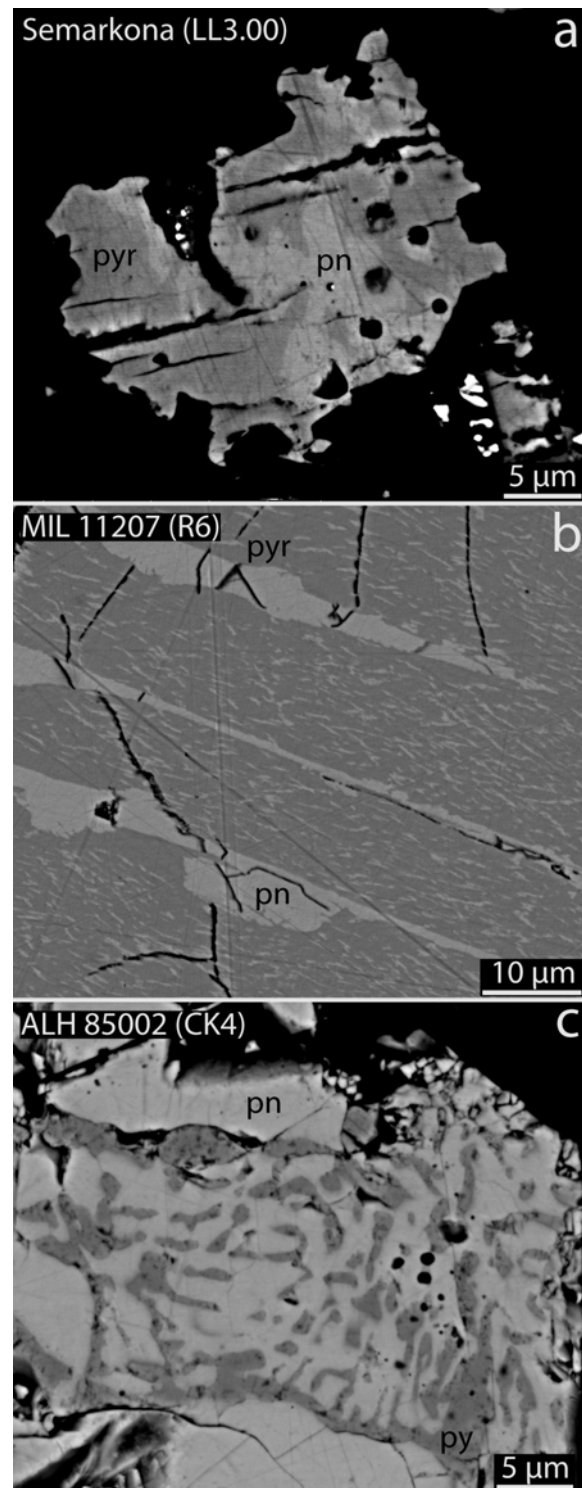


Figure 1. BSE images of pyrrhotite(pyr)-pentlandite (pn) intergrowth textures. Pentlandite blebs in a) Semarkona (LL3.00), pentlandite lamellae and oriented stringers in pyrrhotite in b) MIL 11207 (R6), and islands of pyrite (py) in pentlandite in c) ALH 85002 (CK4).